Available online at www.sciencedirect.com
ScienceDirect
Journal of Power Sources 160 (2006) 116–122
JOURNAL OF POWER SOURCES
www.elsevier.com/locate/jpowsour

Experimental study on the performance of PEM fuel cells with interdigitated flow channels

Wei-Mon Yan [a,*], Sheng-Chin Mei [a], Chyi-Yeou Soong [b], Zhong-Sheng Liu [c], Datong Song [c]

[a] *Department of Mechatronic Engineering, Huafan University, Shih-Ting, Taipei 223, Taiwan, ROC*
[b] *Department of Aerospace and System Engineering, Feng Chia University, Seatwen, Taichung 40724, Taiwan, ROC*
[c] *Institute for Fuel Cell Innovation, National Research Council, 3250 East Mall, Vancouver, BC, Canada V6T 1W5*

Received 25 July 2005; received in revised form 23 January 2006; accepted 24 January 2006
Available online 14 March 2006

Abstract

In this work, the effects of interdigitated flow channel design on the cell performance of proton exchange membrane fuel cells (PEMFCs) are investigated experimentally. To compare the effectiveness of the interdigitated flow field, the performance of the PEM fuel cells with traditional flow channel design is also tested. Besides, the effects of the flow area ratio and the baffle-blocked position of the interdigitated flow field are examined in details. The experimental results indicate that the cell performance can be enhanced with an increase in the inlet flow rate and cathode humidification temperature. Either with oxygen or air as the cathode fuel, the cells with interdigitated flow fields have better performance than conventional ones. With air as the cathode fuel, the measurements show that the interdigitated flow field results in a larger limiting current density, and the power output is about 1.4 times that with the conventional flow field. The results also show that the cell performance of the interdigitated flow field with flow area ratio of 40.23% or 50.75% is better than that with 66.75%.

Keywords: PEM fuel cells; Interdigitated flow channel; Performance test

1. Introduction

Water and thermal management is one of the most important issues in the development of high efficient PEM fuel cell systems, and thus a vast amount of studies on this topic have appeared in the past decade. A few one-dimensional (1-D) models of the water and thermal management along the flow channel or normal to the reactive surface were examined [1–6]. While a number of two-dimensional (2-D) mathematical models of mass transport and electrochemical reactions were used to predict the performance of PEM fuel cells with conventional flow channel design [7–13]. Recently, three-dimensional (3-D) models for simulation of the reactant transport and performance of the fuel cell with conventional flow field were proposed and examined in details [14–18]. Some experimental studies on conventional flow channels have also been conducted in the recent years [19–21].

To effectively improve the gas transport and water and thermal management, Nguyen [22] proposed an interdigitated flow channel design. This interdigitated flow field is different from the conventional flow field in that the interdigitated flow field has baffles in the flow channels. These baffles force the reactant gas in the fuel channel to flow through diffuser and catalyst layers generating the forced convection inside the layers. Firstly, the forced convection in the diffuser layers generates shear stress and help to remove liquid water and heat and thus improve the water and thermal management. Secondly, the forced convection enhances the diffusion of reactant gas inside the catalyst layers, resulting in a better cell performance.

Modeling and simulation of the mass transport phenomena coupled with the electrochemical reaction poses a challenge of the complex flow phenomena in use of the interdigitated flow channels. Several attempts [23–29] have been made to develop 2-D mathematical models for the problem, but the 2-D models are limited in their ability to capture the highly three-dimensional nature of the interdigitated flow field. As to 3-D models, a number of studies have been performed, for example, Dutta et al. [30], Zhou and Liu [31], Natarajan and Nguyen [32], Um and

* Corresponding author. Tel.: +886 2 26632102; fax: +886 2 26633234.
E-mail address: wmyan@huafan.hfu.edu.tw (W.-M. Yan).

0378-7753/$ – see front matter © 2006 Elsevier B.V. All rights reserved.
doi:10.1016/j.jpowsour.2006.01.063

Nomenclature

I	current density (A cm^{-2})
P	power (W)
T	temperature (°C)
V	voltage (V)

Subscripts

cell	fuel cell
in	cathode inlet

Wang [33], Grujicic et al. [34] and Wang and Liu [35]. Due to the limitation of the numerical model for simulation of multi-physics phenomena, the direct measurement is needed to explore the effects of the interdigitated flow field on the cell performance. A few studies [22,23,35–37] have experimentally demonstrated the effectiveness of the interdigitated flow field.

In this work, the influences of flow area ratios and baffle positions upon fuel cell performance are explored experimentally. To the authors' best knowledge, there is no such kind of experimental evidence available in open literature. Understanding of the dependence of cell performance on the flow area ratio and the baffle position is not only necessary for an in-depth understanding of the water and thermal management but also important to the better design of fuel cell systems.

2. Experiment

Fig. 1 presents a schematic diagram of the experimental apparatus. The apparatus consists of a gas supply system, a flow control system, a temperature control system, a humidifier system, an e-load system, a computerized data acquisition system and a test section. In this work, hydrogen on anode side and oxygen (or air) on cathode side were provided from pressurized gas tanks. The fuel gas flow rates are regulated with electric mass flow controller. The drainage valves are used to control the pressure on each side of the cell. To maintain the uniform cell temperature, a heater with an Omega CN76000 PID temperature controller, is employed to heat the unit PEM fuel cell to the desired temperature. In this work, both the anode and cathode fuel gases are humidified by forcing the gases through humidification bottles. The electric load is a semiconductor device that allows high currents to be drawn at low voltages. The load is air-cooled and rated at 600 W. The temperature controllers for the humidification bottles and fuel cell heating elements are also located in the load unit. A Pentium-4 personal computer running

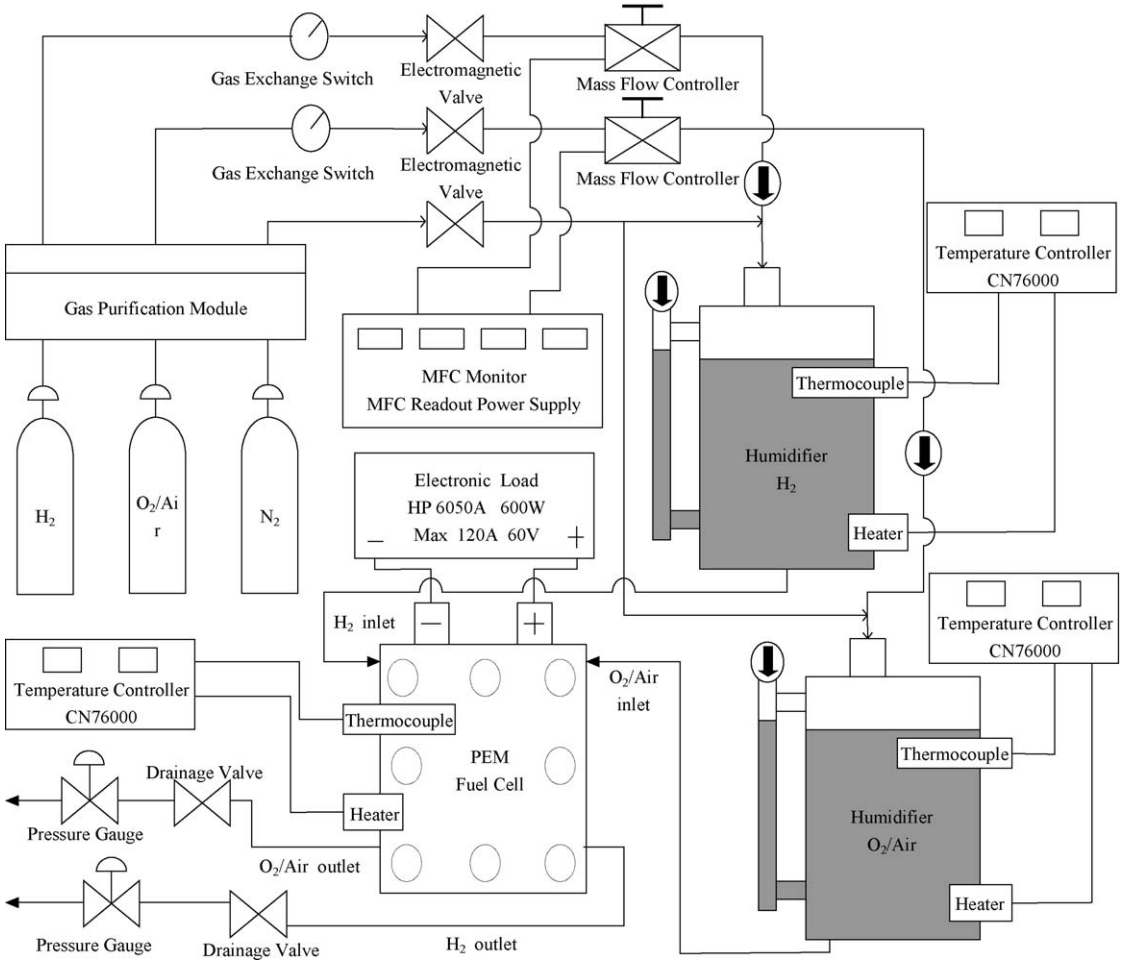

Fig. 1. Schematic diagram of the experimental setup.

Windows XP2000 and a LabView-based software with a variety control, data logging and displaying features is employed for the experimental monitoring and controlling. The computer is connected with the load unit by a GPIB bus. The load unit transmits control signals to the flow rate and temperature controllers.

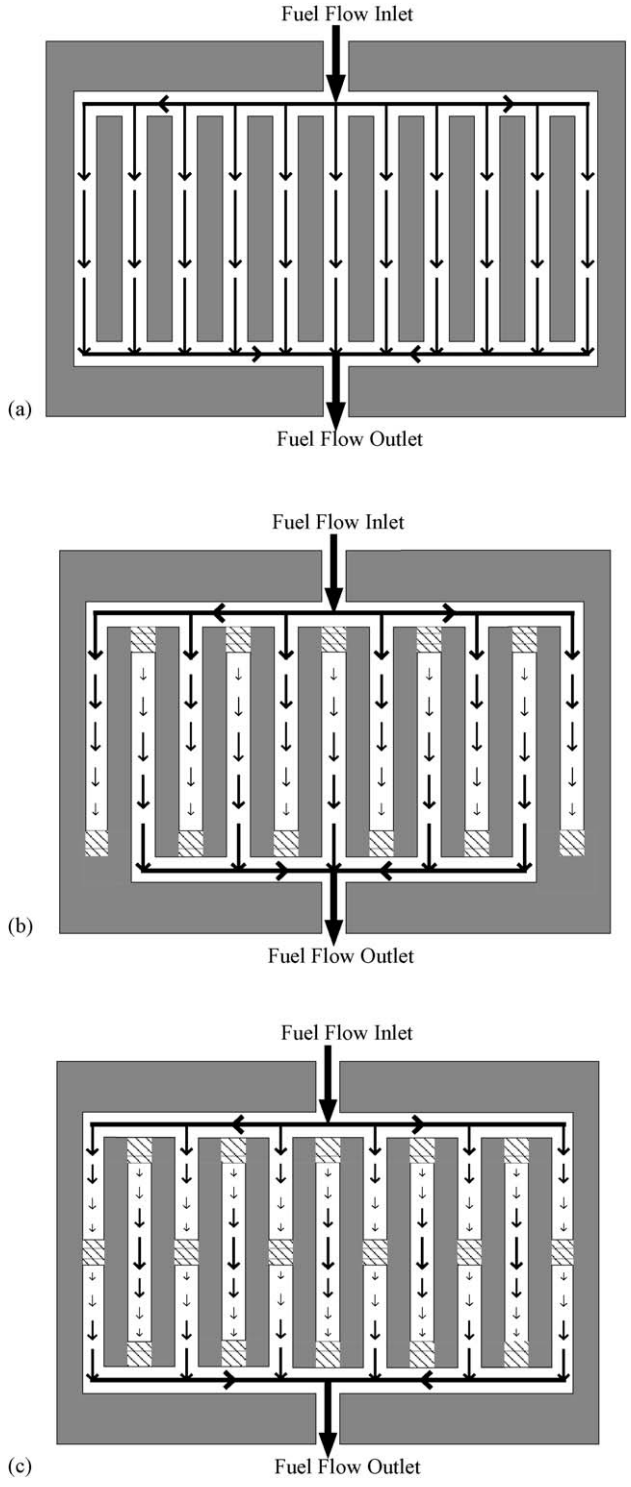

Fig. 2. Schematic diagram of the test models of flow fields. (a) Conventional parallel flow field; (b) interdigitated flow field I with a baffle located at one end of each flow path; (c) interdigitated flow field II with baffles located at the mid-way/ends of each flow path.

In this work, the software permits current density–voltage data to be measured in a galvanostatic (controlled current) or potentialstatic (controlled voltage) mode. The gas flow rates can be controlled as a function of the current drawn, thus keeping stoichiometry constant or a fixed value.

In the present experiment, a GORE-TEX PRIMRA5621 Membrane Electrode Assemblies (MEA) with 198.81 cm^2 active surface area is used. The PEM membrane is of 35 μm in thickness. The catalyst Pt loading is 0.45 mg cm^{-2} (20% Pt/C, E-TEK) on the cathode side and 0.6 mg cm^{-2} on the anode side. The MEA is then sandwiched between two copper current collectors and assembled between graphite plates (POCO Co.) on which fuel distribution channels are machined. In order to examine the effects of flow channel design on the cell performance, three different designs as schematically shown in Fig. 2 are employed for the cathode fuel distributing graphite plates. Fig. 2(a) shows the conventional flow channel pattern without baffle in flow channels. The interdigitated flow channel I (see Fig. 2(b)), is one with a baffle placed at one end of each flow path. Fig. 2(c) presents the interdigitated flow channel II with the baffles located at the mid-way or end of each flow path. For each flow field design, three flow area ratios, 60.22%, 50.75% and 40.23%, are tested. For the cases with the flow area ratio 50.75%, the widths of the flow channel and rib are the same

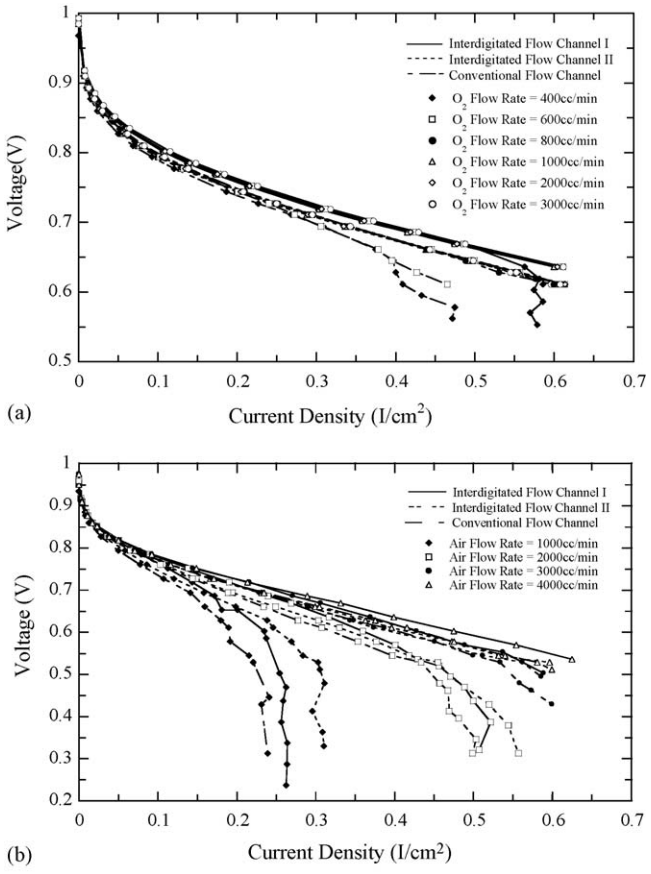

Fig. 3. Effects of flow channel design and cathode fuel flow rate on the cell performance of PEM fuel cells with (a) oxygen and (b) air as the cathode fuel gas.

and equal to 1 mm for the three flow field designs. While for the cases with flow area ratios of 40.23% (or 60.22%), the widths of the flow channel and rib are 0.8 mm (or 1.2 mm) and 1.2 mm (or 0.8 mm), respectively. In addition, the depth and length of the flow channel are kept to be 1 mm and 141 mm, respectively. The flow field of the cathode side consists of 69 parallel flow channel and 68 ribs, while the structure of the Z-type flow field with the flow area ratio 50.75% is used on the anode side.

Before collecting cell performance data, the unit cell is preconditioned by operating them potentiostatically at 0.6 V for a minimum of 24 h. For polarization measurement, the cell operates in the potentialstatic (controlled voltage) mode. Initially, the voltage is set to be 0.975 V and is then decreased by a 0.05 V for each measurement. For each measurement, the output current is the average over 30 s after the initial transient.

3. Results and discussion

As mentioned above, in the present experimental study, one conventional flow channel, and two interdigitated flow fields are considered to examine their effects on cell performance. The detailed operating conditions in this work are described in Table 1. Note that the operating conditions at the anode side are fixed; and the conditions at the cathode side are varied to investigate the parametric effects. As shown in Table 1, the hydrogen with the fixed flow rate of 1500 $cm^3\ min^{-1}$ is used as the reactant fuel on the anode side. The humidification temperature 70 °C is kept on the anode side. This implies that the hydrogen at the inlet is maintained fully saturated. Both the back pressures at the anode and the cathode inlets are 0.96 atm.

Fig. 3 shows the effects of cathode fuel (oxygen) flow rates on the polarization curves (*I–V* curves) for three flow channel designs. The flow area ratio is fixed as 50.75% in the cases considered. It can be seen from Fig. 3 that the PEM fuel cells with the interdigitated flow fields I and II perform better than that with conventional flow field. This confirms the concept that the presence of blockage effect due to baffles in the flow channel enhances the fuel gas transport and, in turn, augments the cell performance. Fig. 3(a) shows that the cell performance of the PEM fuel cell with conventional flow channel increases with the oxygen flow rate when the flow rate rises from 400 $cm^3\ min^{-1}$ to 1000 $cm^3\ min^{-1}$. As oxygen flow rate exceeds 1000 $cm^3\ min^{-1}$, further increase in the flow rate has little influence on the cell performance. However, for the cells with interdigitated flow fields I and II, the effects of the flow rate on the cell performance become insignificant as the flow rates exceed 600 $cm^3\ min^{-1}$ and 400 $cm^3\ min^{-1}$, respectively. This implies that the PEM fuel cells with interdigitated flow field can provide better cell perfor-

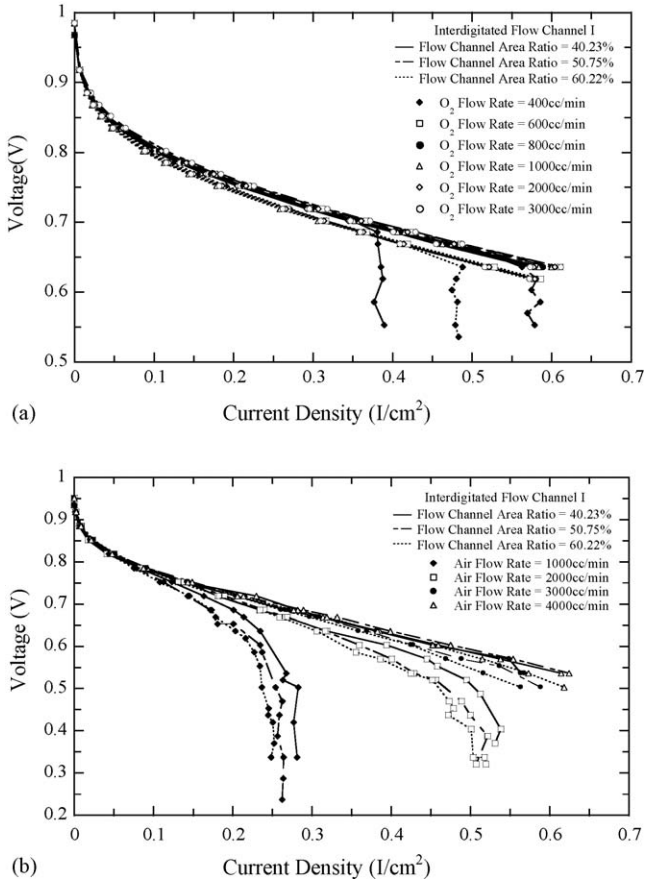

Fig. 4. Effects of flow area ratio and cathode fuel flow rate on the cell performance of PEM fuel cells with the interdigitated flow channel I and (a) oxygen and (b) air as the cathode fuel gas.

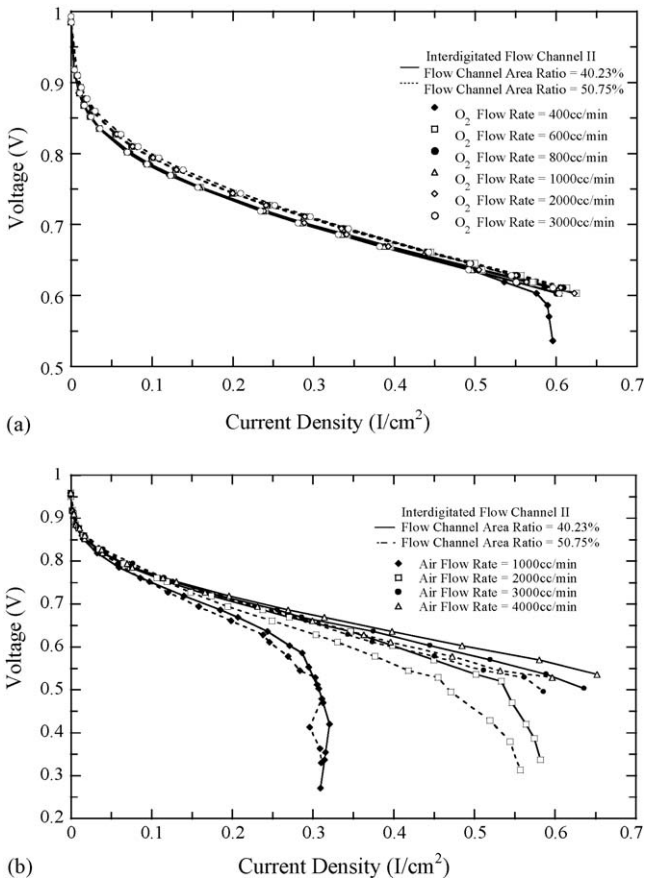

Fig. 5. Effects of flow area ratio and cathode fuel flow rate on the cell performance of PEM fuel cells with the interdigitated flow channel II and (a) oxygen and (b) air as the cathode fuel gas.

Table 1
Operating parameters and conditions used in this work

	Interdigitated flow channel I (with baffles located at the end of the flow channels)		Interdigitated flow channel II (with baffles located at the center and end of the flow channels)		Conventional flow channel	
Hydrogen flow rate ($cm^3\ min^{-1}$)	1500		1500		1500	
Hydrogen humidification temperature (°C)	70		70		70	
	Oxygen[a]	Air[a]	Oxygen[a]	Air[a]	Oxygen[a]	Air[a]
Cathode flow rate ($cm^3\ min^{-1}$)	400		400		400	
	600		600		600	
	800		800		800	
	1000	1000	1000	1000	1000	1000
	2000	2000	2000	2000	2000	2000
	3000	3000	3000	3000	3000	3000
		4000		4000		4000
Cathode humidification temperature (°C)	65		65		65	
Cell temperature (°C)	50		50		50	
Cathode inlet backpressure (atm)	0.96		0.96		0.96	
Anode inlet backpressure (atm)	0.96		0.96		0.96	

[a] Cathode fuel.

mance with a lower oxygen consumption rate. We believe that this performance improvement is caused by more effective fuel transport inside the GDL and the catalyst layer.

At the same operating conditions, a much higher flow rate of air is needed to provide the same amount of oxygen for reaction. Since there is only about one-fifth of the air is oxygen, for the case with a lower airflow rate, the oxygen supply is not enough at a higher current density and a more noticeable mass-transfer overpotenial appears. As air instead of oxygen is used as the cathode reactant fuel, the effects of airflow rate on the cell performance are demonstrated by the polarization curves plotted in Fig. 3(b). It is observed that there is a significant drop in *I–V* curve at a low airflow rate. At a lower airflow rate, i.e. $1000\,cm^3\,min^{-1}$, the PEM fuel cell with interdigitated flow field II shows relatively better cell performance. This means that the PEM fuel cell with interdigitated flow field II can delay the occurrence of the voltage drop at high current density. That is, a higher limiting current density for oxygen starvation is achieved for a PEM fuel cell with the interdigitated flow field II. But at an operating condition with a high airflow rate ($4000\,cm^3\,min^{-1}$), the voltage drop does not occur in the range of the current density considered. It was also observed that the PEM fuel cell with interdigitated flow field shows a better cell performance than that with conventional flow field when the air is used as the cathode fuel reactant.

The flow area ratio, which is defined as the ratio of the flow channel area to the total reacting area of bipolar plate, is one of important design parameters. Here the total reacting area is defined as the sum of the flow channel area and the ribbed area. Fig. 4 presents the influences of the flow area ratios and fuel flow rates on the cell performance of the test cell with interdigitated flow channel I. In Fig. 4(a), the data show that for the low oxygen flow rate of $400\,cm^3\,min^{-1}$, voltage drop occurs at a so-called limiting current density for each flow area ratio due to mass transfer loss. Of the three values of the flow area ratio, the case with flow area ratio 50.75% has the highest limiting current density. But when the oxygen flow rate exceeds $600\,cm^3\,min^{-1}$, the effect of the oxygen flow rate on the cell performance is negligible for various flow area ratios considered. A detailed examination of the experimental data discloses that, under the condition of operating voltage at 0.636 V and oxygen flow rate at $1000\,cm^3\,min^{-1}$, the unit cell power outputs are 71 W, 77 W and 67 W, respectively, for the flow area ratios of 40.23%, 50.75% and 60.22%. This implies that, with the oxygen used as fuel gas, the best cell performance is associated with the flow area ratio of 50.75%. Similar to the result in Fig. 4(a), there is a significant voltage drop in the *I–V* curve for a lower airflow rate ($1000\,cm^3\,min^{-1}$). However, the highest limiting current density corresponds to the flow area ratio 40.23% instead of 50.75%. For a higher flow rate, e.g. $4000\,cm^3\,min^{-1}$, both the flow area ratios 40.23% and 50.75% result in better cell performance. It can be speculated that the optimal flow area ratio for the PEM fuel cells with interdigitated flow fields I and II could be a value between 40% and 50% under the ranges of the present experimental conditions. In fact, a larger flow area ratio leads to the stronger fuel gas transport, which is beneficial to the cell performance. Under this condition, however, the smaller effective rib area would cause a higher contact resistance and in turn degrade the performance. These two counter effects result in a non-monotonic trend of the cell performance and an optimal flow area ratio appears as well.

The location of baffles is one of the important design parameters of bipolar plates. Fig. 5 presents the effects of the flow area ratio and the airflow rate on the cell performance of PEM fuel cells with the interdigitated flow channel II. It is clearly seen that the flow channel with the flow area ratio 40.23% shows a better cell performance than that with 50.75%. In addition, at the same

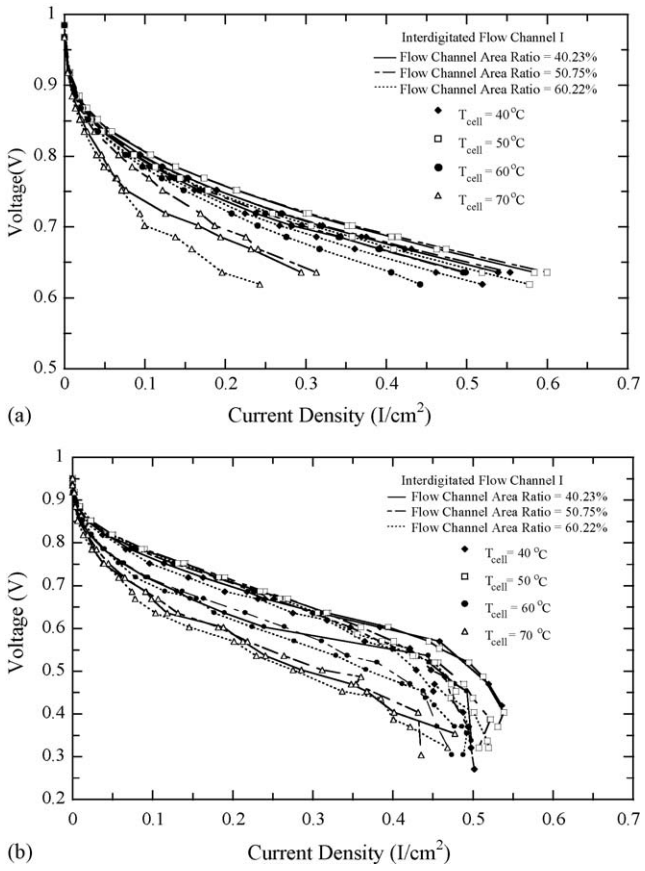

Fig. 6. Effects of flow area ratio and cell temperature on the cell performance of PEM fuel cells with the interdigitated flow channel I and (a) oxygen and (b) air as the cathode fuel gas.

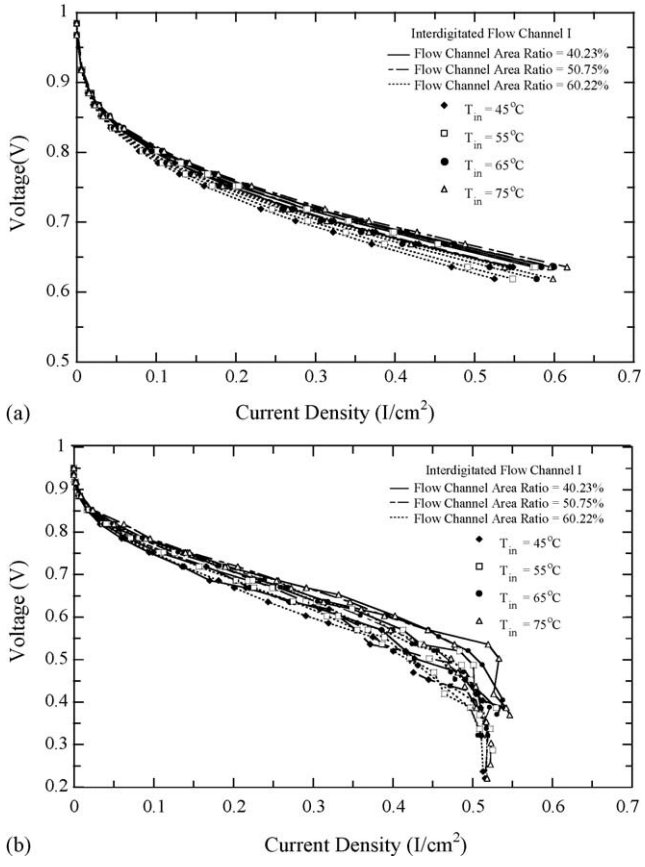

Fig. 7. Effects of flow area ratio and cell temperature on the cell performance of PEM fuel cells with the interdigitated flow channel I and (a) oxygen and (b) air as the cathode fuel gas.

cell performance, a lower air consumption rate is needed for the case with a flow area ratio 40.23%.

The operating temperature also affects the cell performances. Fig. 6 presents the effects of the cell temperature on the cell performance with the interdigitated flow field I. The experiments were carried out with the cathode humidification temperatures fixed at 65 °C. Higher cell temperature may cause higher electrode reaction and transport rates and in turn a higher cell performance. However, the experimental data show a non-monotonical trend. In Fig. 6, the cell performance increases with the cell temperature in the range of 40–50 °C. As the cell temperature exceeds 50 °C, the cell performance drops with an increase in the cell temperature. It implies that the membrane could be dehydrated as the cell temperature over 50 °C). Based on this fact, it seems that there is an optimal cell temperature for the performance of the unit cell, and for the present test cell and experimental conditions, this optimal value lies between 40 °C and 50 °C. In addition, it is noted that the effects of the cell temperature is more significant under the operating conditions of high current density. At low current densities, the performance of the unit cell does not change much with an increase in cell temperature.

For the PEM fuel cell with the interdigitated flow channel I, the effects of the humidification temperature or inlet temperature are shown in Fig. 7. In these cases, the data are measured on the test cell at fixed cell temperature 50 °C and anode inlet temperature 70 °C, which implies that the hydrogen at anode inlet is maintained fully saturated. It is not very similar to the "direct liquid water injection" by Wood et al. [37], but the contained water vapor condensed to liquid water at the lower cell temperature indeed has the effect of humidification. As to the cathode side, humidification temperature 45–75 °C are considered. The measurements presented in Fig. 7 shows a trend of better cell performance can be obtained with higher cathode humidification temperature. Obviously, the fuel gas humidification in the present test has a beneficial effect of preventing the membrane and anode from dehydration. Also, the data reveal that the flow channel area ratio of 50.75% and 40.23% lead to better cell performance.

4. Conclusions

In the present experimental study, the cell performance of PEM fuel cells with conventional and interdigitated flow channel designs has been investigated with the emphasis on the effects of the flow area ratio, and operating temperature. Based on the present test results, the following conclusions can be drawn.

1. Either with oxygen or air as the cathode fuel, the PEM fuel cells with interdigitated flow fields have better performance

than conventional ones. The cells with an interdigitated flow channel require a lower reactant fuel consumption rate as compared with the cells with a conventional flow channel. In addition, the occurrence of the voltage drop or mass transfer loss at higher current density can be delayed for the cells with an interdigitated flow field. The measurements show that the interdigitated flow field results in a larger limiting current density, and the power output is about 1.4 times that with the conventional flow field.

2. The performance of a PEM fuel cell operating with oxygen is better than that with air as the cathode fuel gas. Although the oxygen fraction in air is about one-fifth, the cell performance with five units of airflow rate is still lower than that with one unit of oxygen flow rate. This is due to the chocking effects of nitrogen in the gas diffuser layer and catalyst layer in the cases of air used as the reactant fuel gas.
3. Regarding the PEM fuel cells with interdigitated flow field, the flow area ratio between 40% and 50% lead to a better cell performance than that with 60%.
4. The cell performance is enhanced as the cell temperature goes up from 40 °C to 50 °C. As the cell temperature exceeds 50 °C, increasing the cell temperature leads to degradation in the cell performance. The dehydration of membrane and the reduction in the active area of the catalyst surface at high temperatures are believed to be the major reasons. The present experimental results demonstrate the existence of an optimal operating condition of the cell temperature.
5. In the present test cases, the data reveals that the anode fuel gas (hydrogen) with saturated condition of humidification temperature and increase in the cathode humidification temperature both enhance the cell performance with a beneficial effect of preventing anode/membrane from dehydration.

Acknowledgements

The study was supported by the National Science Council, the Republic of China, through the grants NSC 93-2212-E-211-011, NSC 92-2623-7-002-006-ET, 92-2212-E-035-027 and NSC 92-2212-E-002-096. In addition, the partial supports from ITRI and MOEA are also appreciated.

References

[1] T.F. Fuller, J. Newman, J. Electrochem. Soc. 140 (1993) 1218.
[2] T.V. Nguyean, R.E. White, J. Electrochem. Soc. 140 (1993) 2178.
[3] V. Gurau, F. Barbir, H. Liu, J. Electrochem. Soc. 147 (2000) 2468–2477.
[4] W.M. Yan, F. Chen, H.Y. Wu, C.Y. Soong, H.S. Chu, J. Power Sources 129 (2004) 127–137.
[5] F. Chen, Y.G. Su, C.Y. Soong, W.M. Yan, H.S. Chu, J. Electroanal. Chem. 566 (2004) 85–93.
[6] F. Chen, H.S. Chu, C.Y. Soong, W.M. Yan, J. Power Sources 140 (2005) 243–249.
[7] A.C. West, T.F. Fuller, J. Appl. Electrochem. 26 (1996) 57.
[8] V. Gurau, H. Liu, S. Kakac, AIChE J. 44 (1998) 2410.
[9] H.P. Van Bussel, F.G. Koene, R.K. Mallant, J. Power Sources 71 (1998) 218–222.
[10] F. Chen, Z. Wen, H.S. Chu, W.M. Yan, C.Y. Soong, J. Power Sources 128 (2004) 125–134.
[11] W.M. Yan, C.Y. Soong, F. Chen, H.S. Chu, J. Power Sources 125 (2004) 27–39.
[12] W.M. Yan, C.Y. Soong, F. Chen, H.S. Chu, J. Power Sources 143 (2005) 48–56.
[13] J.H. Jang, W.M. Yan, C.C. Shih, J. Power Sources, in press.
[14] T.C. Jen, T. Yan, S.H. Chan, Int. J. Heat Mass Transfer 46 (2003) 4157–4168.
[15] A. Kumar, R.G. Reddy, J. Power Sources 113 (2003) 11–18.
[16] S. Mazumder, J.V. Cole, J. Electrochem. Soc. 150 (2003) A1503–A1509.
[17] S. Mazumder, J.V. Cole, J. Electrochem. Soc. 150 (2003) A1510–A1517.
[18] T. Berning, N. Njilali, J. Electrochem. Soc. 150 (2003) A1589–A1598.
[19] H. Dohle, R. Jung, N. Kimiaie, J. Mergel, M. Muller, J. Power Sources 124 (2003) 371–384.
[20] D. Hyun, J. Kim, J. Power Sources 126 (2004) 98–103.
[21] K. Tuber, A. Oedegaard, M. Hermann, C. Hebling, J. Power Sources 131 (2004) 175–181.
[22] T.V. Nguyen, J. Electrochem. Soc. 143 (1996) L103.
[23] W. He, J.S. Yi, T.V. Nguyen, AIChE J. 46 (2000) 2053.
[24] J.S. Yi, T.V. Nguyen, J. Electrochem. Soc. 146 (1999) 38.
[25] A. Kazim, H.T. Liu, P. Forges, J. Appl. Electrochem. 29 (1999) 1409.
[26] C.Y. Wang, P. Cheng, Int. J. Heat Mass Transfer 39 (1996) 3619.
[27] H.C. Liu, W.M. Yan, C.Y. Soong, F. Chen, J. Power Sources 142 (2005) 125–133.
[28] C.Y. Soong, W.M. Yan, C.Y. Tzeng, H.C. Liu, F. Chen, H.S. Chu, J. Power Sources 143 (2005) 36–47.
[29] J.H. Jang, W.M. Yan, H.Y. Li, Y.C. Chou, J. Power Sources, in press.
[30] S. Dutta, S. Shimpalee, J.W. Van Zee, J. Appl. Electrochem. 30 (2000) 135.
[31] T. Zhou, H. Liu, Int. J. Transport Phenom. 3 (2001) 177.
[32] D. Natarajan, T.V. Nguyen, J. Power Sources 115 (2003) 66–80.
[33] S. Um, C.Y. Wang, J. Power Sources 125 (2004) 40–51.
[34] M. Grujicic, C.L. Zhao, K.M. Chittajallu, J.M. Ochterbeck, Mater. Sci. Eng. B 108 (2004) 241–252.
[35] L. Wang, H. Liu, J. Power Sources 134 (2004) 185–196.
[36] M.S. Wilson, F.H. Garzon, K.E. Sickafus, S. Gottesfeld, J. Electrochem. Soc. 140 (1993) 2872.
[37] D.L. Wood, J.S. Yi, T.V. Nguyen, Electrochim. Acta 43 (1993) 3795.